# Magmatic Evolution, Mineralization and Alteration of the Red Chris Copper-Gold Porphyry Deposit, Northwestern British Columbia (NTS 104H/12W)

**J.R. Norris,** Mineral Deposit Research Unit, University of British Columbia, Vancouver, BC, jnorris@eos.ubc.ca

**C.J.R. Hart,** Mineral Deposit Research Unit, University of British Columbia, Vancouver, BC

**R.M. Tosdal,** Mineral Deposit Research Unit, University of British Columbia, Vancouver, BC

**C. Rees,** Imperial Metals Corporation, Vancouver, BC

Norris, J.R., Hart, C.J.R., Tosdal, R.M. and Rees, C. (2011): Magmatic evolution, mineralization and alteration of the Red Chris copper-gold porphyry deposit, northwestern British Columbia (NTS 104H/12W); *in* Geoscience BC Summary of Activities 2010, Geoscience BC, Report 2011-1, p. 33–44.

## Introduction

The Red Chris porphyry Cu-Au deposit in British Columbia has geological features that are typical of both alkalic and calcalkalic porphyry deposit types. Quartz-vein stockworks, typically absent in most alkalic porphyries, characterize the best mineralized zones at Red Chris. Intense late-stage clay alteration, such as illite and kaolinite, is present at Red Chris. Perhaps the most curious feature is the widespread and intense late carbonate alteration (Baker et al., 1999), which is not a common feature of porphyry Cu systems (Seedorff et al., 2005). Nonetheless, Red Chris is hosted in monzonitic rocks, has characteristic hematite alteration, and has the high Au grades typical of BC alkalic porphyry deposits (Newell and Peatfield, 1995; Baker et al., 1999; Holliday and Cooke, 2007).

The Red Chris deposit is in northwestern BC (Figure 1), approximately 80 km south of the town of Dease Lake and 12 km east of the Stewart-Cassiar Highway (Highway 37). It is accessed by a 23 km gravel road. The deposit is situated at latitude 57°42'N and longitude 129°47'W, in NTS area 104H/12W. The rock units, mineralization, associated veins and alteration at Red Chris were previously described by Schink (1977), Ash et al. (1995), Blanchflower (1995) and Baker et al. (1999).

The property has been explored intermittently by several companies since the mid-1950s, with a hiatus between 1981 and 1994 when more focused drill projects dominated (Newell and Peatfield, 1995). Exploration drilling campaigns continued until 2005 and resulted in a calculated open-pit reserve by bcMetals Corporation. This reserve (proven and probable) has been recently updated to

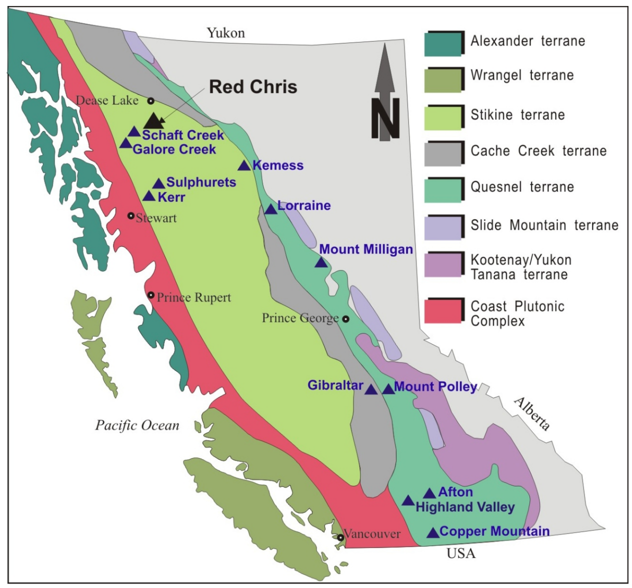


**Figure 1.** Major tectonic terranes and associated Mesozoic porphyry deposits of the Canadian cordillera in British Columbia.

301.5 million tonnes grading 0.359% Cu and 0.274 g/t Au (Imperial Metals Corporation, 2010). Following a takeover by Imperial Metals Corporation in February 2007, drilling between 2007 and 2009 targeted deeper mineralization in the 'East zone' and 'Main zone', resulting in new dimensions to the potential shape, depth, size and grade of the Red Chris deposit. The most notable results came from the East zone: 1) RC07-335 intersected 1024.1 m of 1.01% Cu, 1.26 g/t Au and 3.92 g/t Ag over the entire length of the hole (Imperial Metals Corporation, 2007), and 2) RC09-350 intersected 152 m of 4.12% Cu, 8.83 g/t Au and 10.46 g/t Ag at a depth of 504 m (Gillstrom and Robertson, 2010). More importantly, these deep drillholes demonstrated vertical continuity at Red Chris and had significant implications for further exploration and mine planning. An updated resource estimate of 619 million tonnes (measured and indicated) at 0.38% Cu and 0.36 g/t Au (at 0.1% Cu-equivalent cut-off, with inferred resources of more than 619 million

***Keywords:*** *Stikine terrane, copper, porphyry deposits, alteration, Red Chris*

*This publication is also available, free of charge, as colour digital files in Adobe Acrobat® PDF format from the Geoscience BC website: http://www.geosciencebc.com/s/DataReleases.asp.*

tonnes at 0.30% Cu and 0.32 g/t Au) was released in May 2010 (Gillstrom and Robertson, 2010). On a broader scale, results from these deep drillholes indicate significant potential for high Au and Cu grades in BC's alkalic porphyry systems. Giroux and Bellamy (2004) reported inferred resources at the Far West and Gully zones containing 76.8 million tonnes of 0.17 % Cu and 0.33 g/t Au (at 0.1 % Cu-equivalent cut-off) and 230.3 million tonnes of 0.22 % Cu and 0.20 g/t Au (at 0.1 % Cu-equivalent cut-off), respectively.

Results from the 2007 drilling program encouraged a joint research project between the Mineral Deposit Research Unit at the University of British Columbia, Imperial Metals Corporation and Geoscience BC. Observations and results presented herein are from investigations of the second field season at the Red Chris deposit in the summer of 2010, when 11 833 m of diamond-drill core were logged. Results presented here build upon observations of Norris et al. (2010).

This paper focuses on increasing the understanding of the magmatic evolution, mineralization styles and alteration of the deposit, with particular emphasis on the deeper parts of the East zone. Specifically, the emphasis is along a 500 m long section trending N50 E, where the nature of the intrusive rocks, mineralization, veins and alteration were investigated in eight diamond-drill holes in 2010. Additionally, a diamond-drill hole studied in 2009 (RC07-335) lies on this section (Norris et al., 2010). Samples were taken roughly every 50 m as 10–15 cm slabs of previously cut drillcore, for a total of 324 samples along the N50E section.

## Tectonic Setting

Much of BC is underlain by several tectonic blocks that were accreted to the growing margin of western North America during the Mesozoic. Three of these accreted terranes, the Quesnel terrane (or Quesnellia), the Stikine terrane (or Stikinia) and the Cache Creek terrane form most of the Intermontane Belt that underlies much of central BC (Monger and Price, 2002). Stikinia and Quesnellia are dominated by Late Triassic to Early Jurassic island-arc terranes that host most of BC's porphyry deposits and are separated from each other by the intervening Cache Creek terrane (McMillan et al., 1995; Figure 1). These dominantly Late Triassic volcanic island-arc terranes, which have similar compositions and stratigraphy, formed outboard from the western North American continental margin and were subsequently accreted to the margin during the Early Jurassic (Monger and Price, 2002). Porphyry Cu deposits within Quesnellia and Stikinia formed largely in the latest Triassic prior to accretion, but some deposits continued to form into the Middle Jurassic (e.g., Mount Milligan; McMillan et al., 1995). The Late Triassic to Early Jurassic Red Chris porphyry deposit is hosted in the Late Triassic to Early Jurassic arc and arc-marginal sedimentary rocks in the northern portion of Stikinia.

## Regional Geology

There are three main geological packages in the Red Chris area: the late Triassic Stuhini Group, the late Triassic Red stock and the Middle Jurassic Bowser Lake Group (Figure 2). The Stuhini Group (**LTrS**) consists of Late Triassic volcanic and volcanically derived sedimentary rocks that form part of Stikinia. These arc-volcanic rocks (**LTrSb**) are dominated by augite-phyric basaltic pillowed flows and flow breccias to basaltic andesite (Ash et al., 1995). The volcanic rocks are intercalated with fine-grained mafic-derived volcaniclastic siltstone, siliceous siltstone and feldspathic sandstone (**LTrSss**), on the order of metres to tens of metres in apparent thickness.

Plutonic rocks of the Late Triassic Red stock (**LTrEJmd**) intruded the Stuhini Group and form an east-northeast-trending, 4.5 by 1.5 km body (Ash et al., 1995; Ferreira, 2009). The stock consists of medium- to coarse-grained hornblende-plagioclase–porphyritic monzodiorite (Ash et al., 1995). A monzonite sample taken at a depth of ~105 m in drillhole RC95-224 gave a U-Pb zircon crystallization age of 203.8 ±1.3 Ma (Freidman and Ash, 1997). The South Boundary fault truncates the Red stock at its southern margin and juxtaposes the plutonic rocks against the Bowser Lake Group.

Sedimentary rocks of the Middle Jurassic Bowser Lake Group (**MJB**) outcrop south of the South Boundary fault. These marine clastic sedimentary rocks, belonging to the Ashman Formation, were deposited unconformably on top of the Late Triassic volcanic and plutonic rocks. The sedimentary rocks represent the basal unit of the Bowser Lake Group and are composed of siltstone, chert-pebble conglomerate and sandstone (Evenchick and Thorkelson, 1993).

## Deposit Geology

The Red Chris deposit consists of several mineralized zones: the Main, East, Far West and Gully zones (Figure 2). Currently only the Main and East zones host measured and indicated resources. The Main zone has a larger areal extent than the East zone, and their centres are ~600 m apart. Both Main and East zones are vertical to subvertical, apparent pipe-like orebodies that are bounded to the south by the general east-northeasterly-trending faults in the region (Collins et al., 2004).

The high-grade mineralized zones are hosted entirely within the Red stock, a plagioclase-hornblende–porphyritic monzodiorite that probably consists of multiple intrusive phases. The stock is cut by several late-stage felsic dikes.

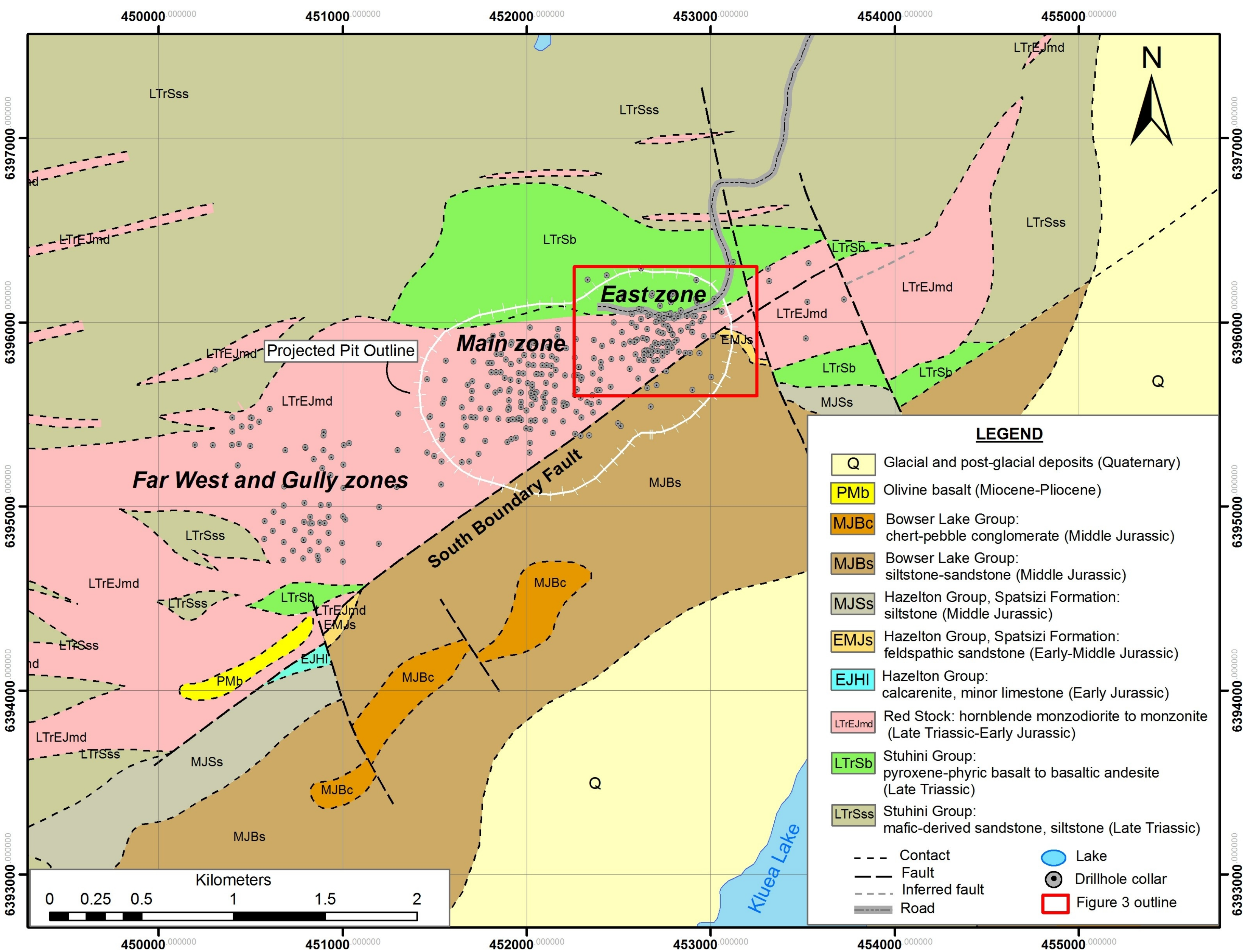


**Figure 2.** Regional-scale geology of the Red Chris deposit, northwestern British Columbia (from Imperial Metals Corporation). The planned open-pit outline is highlighted in white.

The drillholes logged during this study are highlighted in yellow on the drillhole plan (Figure 3).

## Rock Units

### Intrusive Rocks

Historically, the composite Red stock in the East zone (see Schink, 1977) was considered to comprise main and late intrusive phases, both of which are cut by postmineral dikes. However, this study has observed that there is no discernible textural difference between the main phase and late phase of Schink (1977). Only a few crosscutting relationships between intrusive phases are preserved. Most of these contacts appear to have been reactivated by later faults and are intensely carbonate cemented. There are apparent changes in size and density of plagioclase and hornblende phenocrysts in addition to minor textural changes in the groundmass; however, these changes do not distinguish separate intrusive phases.

The Red stock intrusive suite is monzonite to monzodiorite in composition (Ash et al., 1995). However, it is uncertain if the K-feldspar in the groundmass is primary or of secondary origin due to extensive alteration. Throughout this paper, the Red stock will be referred to as a monzodiorite.

The Red stock is medium grey with phenocrysts of plagioclase and hornblende in a very fine grained groundmass (Figure 4a). The groundmass typically accounts for 40% of the rock and consists of anhedral microcrystalline K-feldspar and minor quartz (Schink, 1977). The feldspar phenocrysts are generally buff-white, 2–4 mm euhedral to subhedral crystals (Figure 4b–d). Hornblende phenocrysts are altered to secondary biotite and sericite, making the primary texture difficult to ascertain, but are typically euhedral, 2–10 mm crystals with distinct crystal boundaries (Figure 4b–d). The phenocrysts are randomly oriented within the grey aphanitic groundmass (Schink, 1977). Estimated visually, phenocryst abundance typically varies between 15 and 30%, but can be as low as 5% and as high as 45% (Figure 4a–d).

### Stuhini Group Volcanic Rocks and Associated Sedimentary Rocks

The Stuhini Group volcanic and related sedimentary rocks occur as septa within the Red Stock, as well as the external host rocks. They are typically medium to dark green, as

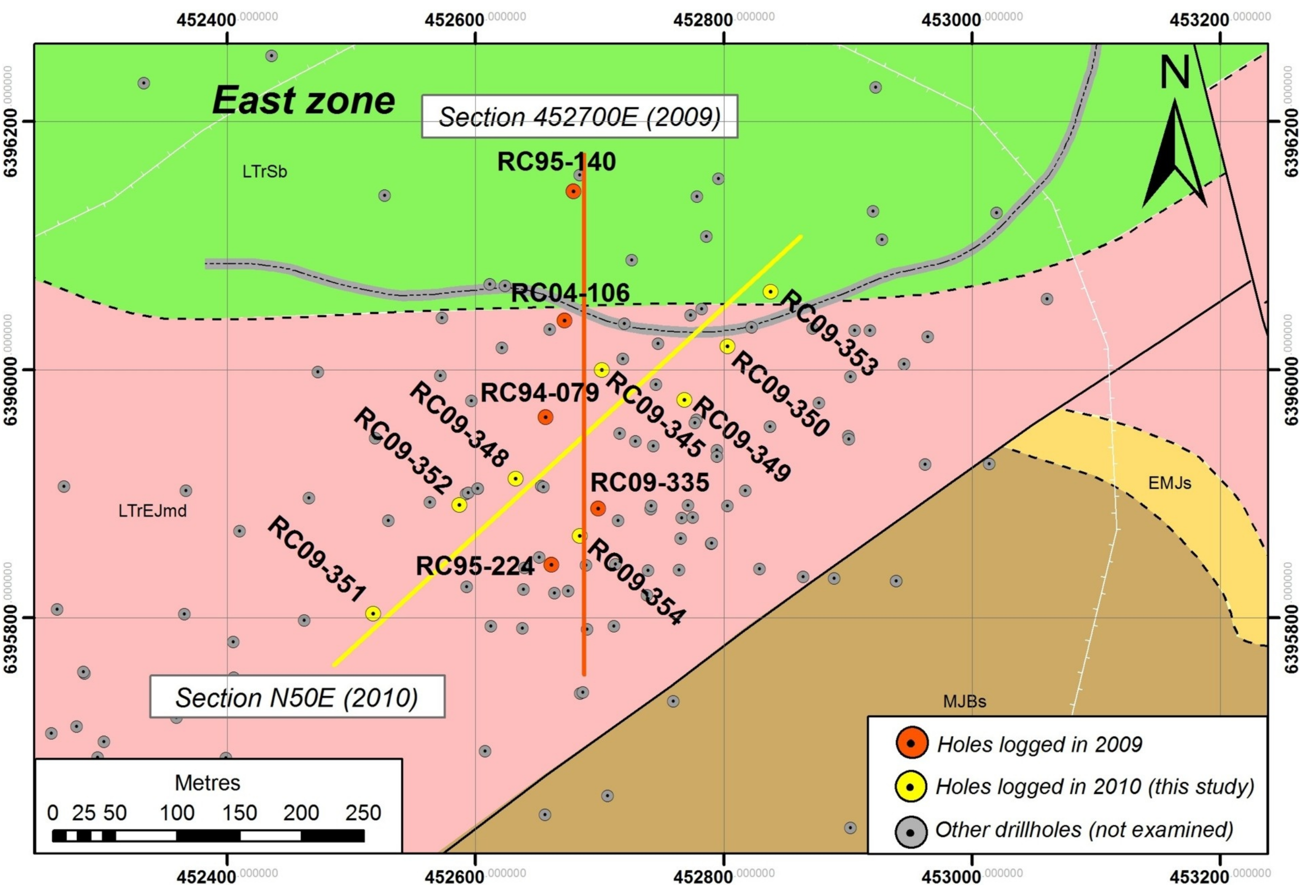


**Figure 3.** Location of N50E cross-section (±85 m) across the East zone of the Red Chris deposit, northwestern British Columbia. Drillholes examined in 2010 and the N50E cross-section are in yellow; drillholes examined in 2009 and section 452700E (discussed in Norris et al, 2010) are in orange. Geology and projected pit outline as per Figure 2.

well as dark brown and locally pale orange near zones of K-silicate alteration. The volcanic rocks are fine grained with local clasts up to 3 mm in diameter, abundant <1 mm microfractures filled with dark black minerals (probably chlorite) and locally pyrite and chalcopyrite. Sparse carbonate and quartz veins cut the Stuhini Group rocks. This unit occurs as isolated, 0.3–30 m thick 'rafts' within the Red stock monzodiorite, below 500 m depth on the flanks of the East zone.

### Postmineral Dikes

Two types of 1–20 m wide (measured in drillcore), diorite to monzodiorite dikes intrude the Red stock. The amygdaloidal monzodiorite and biotite diorite dikes make up <2% of the stock, are not mineralized and are cut by minor, late, buff-white carbonate veins. The amygdaloidal monzodiorite dikes are beige to locally light green and very fine grained, with carbonate>quartz amygdules 2–10 mm in size. Euhedral hornblende phenocrysts (<3%), up to 4 mm long, are altered to clay and/or chlorite. The biotite diorite dikes are light to medium green and very fine grained, with up to 10% hornblende and/or biotite phenocrysts, up to 5 mm long, that are locally altered to clay and/or chlorite. These dikes occur throughout the Red stock, yet are mostly located between 400 and 800 m in depth.

## Alteration

Alteration in the East zone along section line N50E is dominantly potassic (herein called K-silicate alteration) and is overprinted by clay alteration (Figure 5). These rocks were previously recognized as hosting sericite alteration. 'Sericite' is a field term widely used to describe alteration to fine-grained hydrous white mica minerals and may include muscovite, pyrophyllite, paragonite, phlogopite and occasionally illitic mica and interlayered disordered micas with other sheet-structured minerals such as montmorillonite, chlorite and vermiculite (Meyer and Hemley, 1967). Results of shortwave-infrared spectroscopy, using the Analytical Spectral Devices (ASD) TerraSpec™ analyzer, on samples from the 2009 field season identified the dominant 'sericitic' zone clay alteration minerals as illite and lesser kaolinite. Minor chlorite and moderate pervasive carbonate, as ankerite-dolomite, are associated with the illite-

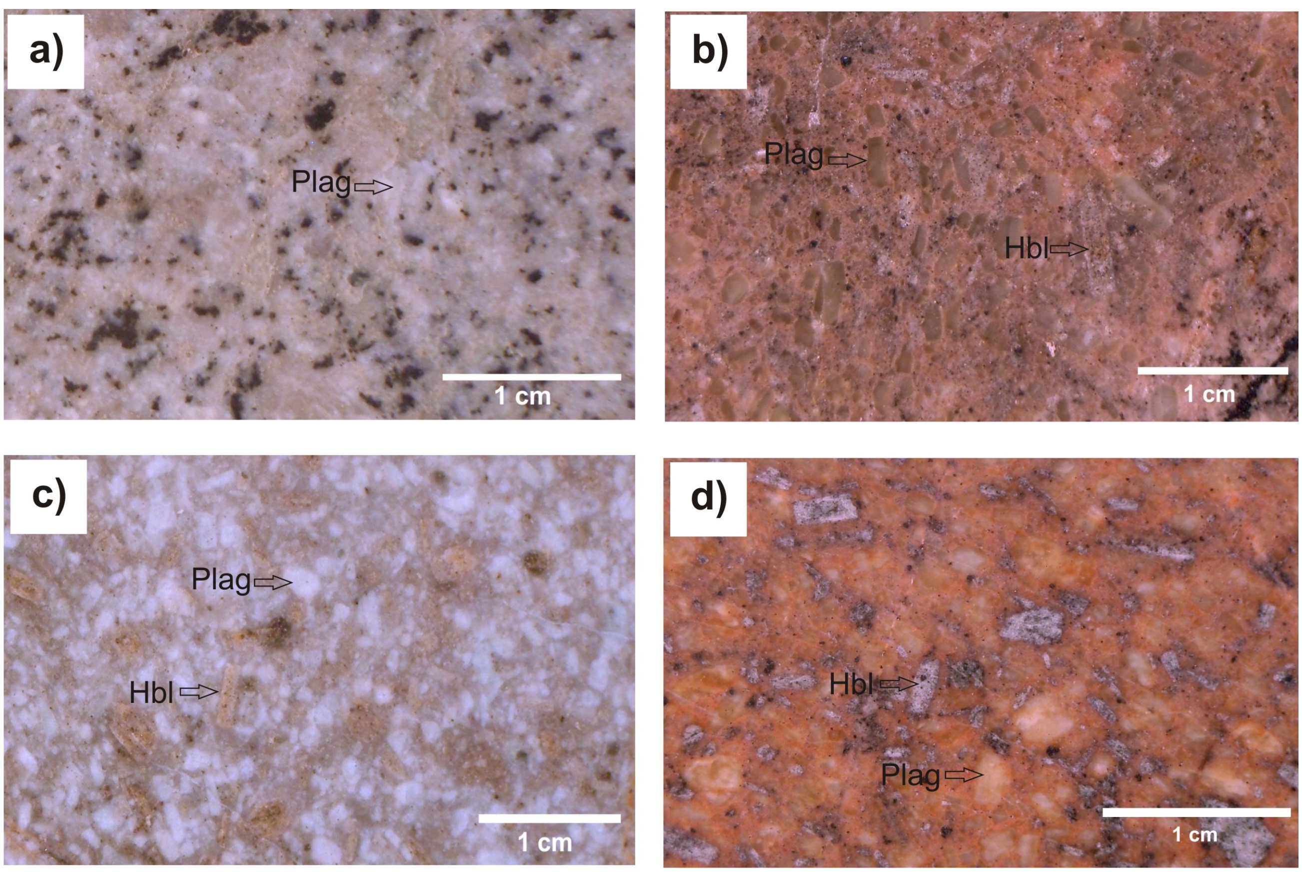


**Figure 4**. Examples of the Red stock taken from diamond-drill holes on the Red Chris deposit, northwestern British Columbia, illustrating the variability in phenocryst size and abundance (reproduced from Norris et al., 2010): **a)** 10% plagioclase (Plag), up to 2 mm in length, and mafic minerals altered to hematite, drillhole RC79-003 (51.52 m); **b)** 15% plagioclase, up to 4 mm in length, altered to illite-kaolinite and 10% hornblende (Hbl), up to 1 cm in length and altered to illite-kaolinite, drillhole RC106-038 (405.51 m); **c)** 25% plagioclase, up to 4 mm in length, and 5% hornblende, up to 7 mm in length, drillhole RC335-036 (461.90 m). **d)** 10% plagioclase, up to 3 mm in length, and 15% hornblende, up to 5 mm in length, drillhole RC224-006 (124.48 m). Drillhole locations are shown on Figure 3.

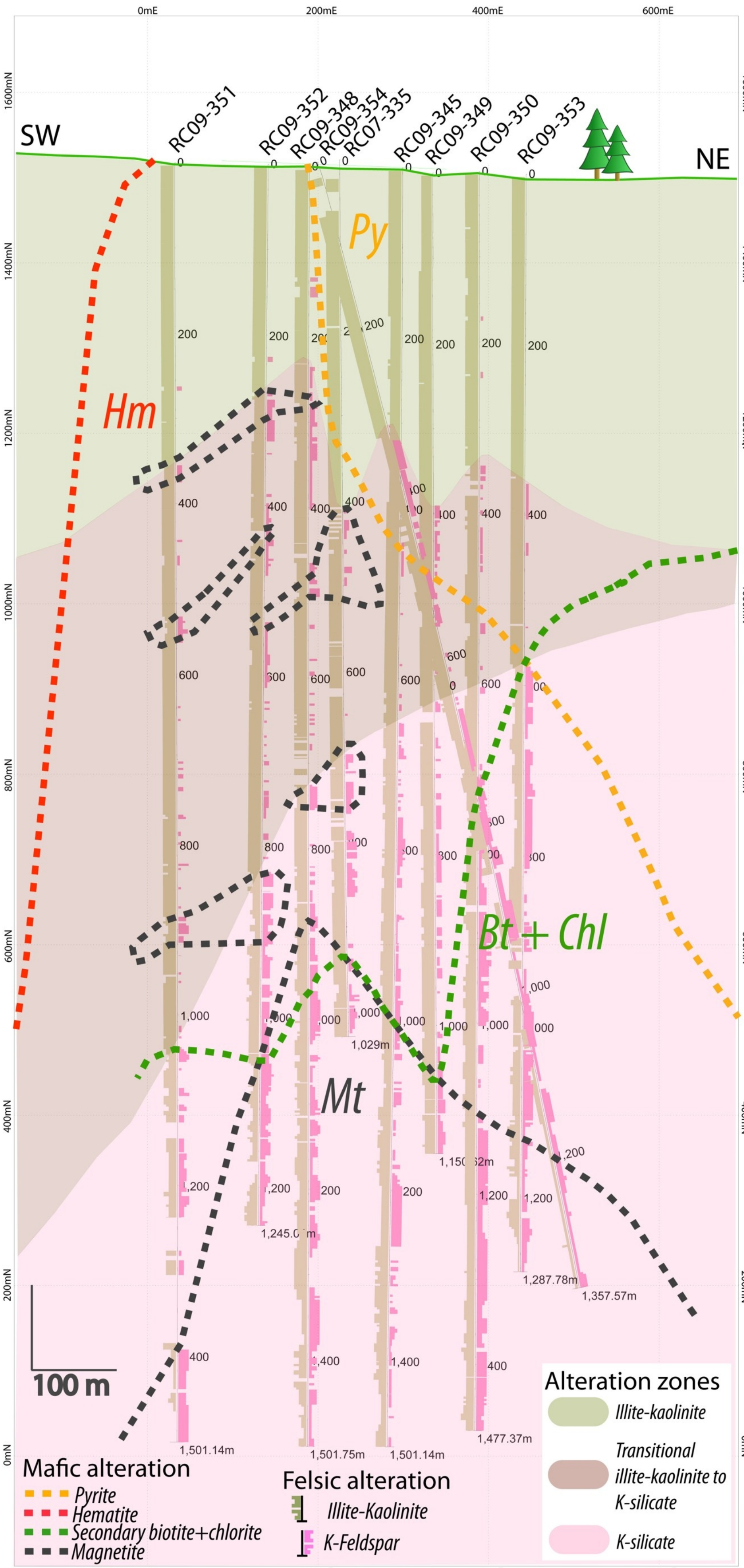
SW
NE
RC09-351
RC09-352
RC09-348
RC09-354
RC07-335
RC09-345
RC09-349
RC09-350
RC09-353
0mE
200mE
400mE
600mE
1600mN
1400mN
1200mN
1000mN
800mN
600mN
400mN
200mN
0mN
Py
Hm
Bt + Chl
Mt
100 m
1,029m
1,245.0 m
1,287.78m
1,357.57m
1,501.14m
1,501.75m
1,501.14m
1,477.37m
Alteration zones
Illite-kaolinite
Transitional illite-kaolinite to K-silicate
K-silicate
Mafic alteration
Pyrite
Hematite
Secondary biotite+chlorite
Magnetite
Felsic alteration
Illite-Kaolinite
K-Feldspar

kaolinite clay alteration. Throughout this paper, the 'sericite' alteration overprint will be referred to as illite-kaolinite.

The K-silicate–dominant alteration zone has a broadly arching geometry, deepest in the westernmost portion of the section (~1000 m depth) and shallowest in the easternmost (~600 m depth). The shallower portions of K-silicate alteration are overprinted by illite-kaolinite alteration, making it difficult to determine the original extent of the K-silicate zone. A transitional zone of weak, residual K-silicate alteration with a moderate to strong illite-kaolinite overprint occurs directly above the intense K-silicate zone and below a zone of intense illite-kaolinite alteration. The upper contact of the transitional zone is irregular, varying in depth between 200 and 400 m (Figure 5).

The K-silicate alteration zone is characterized by secondary biotite, magnetite and texturally destructive K-feldspar that replaced the groundmass and primary plagioclase feldspar phenocrysts (Figure 6a, b). Baker et al. (1999) noted that the porphyritic igneous texture may be completely destroyed by fine-grained orthoclase and albitic feldspar ($Ab_{80–94}$; Schink, 1977). Primary mafic minerals were replaced by secondary biotite and magnetite, and locally by later chlorite (Figure 6c); locations in which they dominate are mapped along section line N50E (heavy dashed lines in Figure 5). Intense secondary biotite and chlorite occur below a depth of 950 m in the eastern portion of the section and at 600 m in the western portion, creating a sharp boundary between holes RC09-349 and RC09-350. A localized zone of moderate secondary biotite and chlorite alteration, occurring in holes RC07-335 and RC09-348 at depths of 400 and 450 m, respectively, is continuous to the west through holes RC09-352 and RC09-351 at a depth of 800 m. Chlorite is present in minor amounts within the mafic sites above the strong and moderate alteration zones and extending to the surface.

Anhydrite veins are part of the mineral association that defines the K-silicate alteration zone. Generally occurring below 1000 m in depth, anhydrite occurs as medium purple to lavender veins where the monzodiorite is visibly K-silicate altered. In areas of weak to moderate illite-kaolinite overprinting, the anhydrite is pale pink to peach. Anhydrite is absent in zones of intense illite-kaolinite alteration, perhaps no longer visible due to exploitation by later quartz veins. Moderate anhydrite veining occurs deepest in the centre of the East zone (depth of 1100 m in drillholes RC09-345, RC09-348, RC09-349 and RC09-354) and shallowest on the flanks of the zone (800 m depth in RC09-350, RC09-351 and RC09-354). Trace epidote is associated with anhydrite veins and also within mafic sites of the freshest looking monzodiorite, below a depth of 1100 m on the flanks of the East zone. Epidote is not observed in the centre of the East zone, in drillhole RC09-345. The occurrence of epidote may indicate that zones of propylitic alteration flank the K-silicate core of the East zone.

In the illite-kaolinite zone, illite and kaolinite pervasively alter both plagioclase and K-feldspars, hornblende phenocrysts and secondary biotite of both the primary and K-silicate–altered monzodiorite to buff-white, pale orange (ankerite-dolomite) and locally pale green (illite; Figure 6d, e). Throughout the illite-kaolinite zone, pervasive but minor hematite occupies the mafic sites and has both sharp and diffuse crystal boundaries. The hematite is very fine grained and dark grey to maroon. Pyrite within the illite-kaolinite zone dominates in the upper eastern portion of the section, occurring as very fine to fine-grained anhedral crystals occurring preferentially within the mafic crystal sites. Magnetite associated with the K-silicate alteration zone is altered to hematite by the illite-kaolinite alteration fluids. Pervasive carbonate alteration is spatially associated with the illite-kaolinite alteration in the upper portions of the section. Baker et al. (1999) reported a ferroan-dolomite composition for this carbonate alteration (Figure 6e, f). The presence of pyrite, hematite and magnetite within the mafic sites has been mapped along section line N50E (Figure 5). Pyrite within the mafic sites dominates in the eastern portion of the section, occurring at a depth of 580 m in RC09-353 (easternmost drillhole) and gradually at shallower depths westward toward RC07-348, where pyrite occurs in the mafic sites in the upper 10 m of the hole. Immediately below the pyrite-dominant zone, hematite is the dominant oxide in the mafic sites, extending to a depth of 900 m depth in RC09-348, marking the apex of a deeper, magnetite-dominant zone. Moderate to abundant amounts of magnetite occur within the mafic sites below this apex and at gradually deeper depths towards the flanks of the East zone. This zone occurs at a depth of ~1150 m in the eastern portion of the section and at 1100–1400 m in the west, with its apex at 950 m in hole RC09-348. Localized isolated pods of magnetite as the dominant oxide in the mafic sites occur throughout the hematite-dominant zone, likely reflecting areas with a less intense illite-kaolinite alteration overprint. A zone of nearly equal hematite and magnetite within the mafic sites indicates a transitional zone between depths of 550 and 1100 m in the easternmost part of the section, in drillholes RC09-353 and RC09-350.

◄

**Figure 5.** Cross-section N50E showing alteration of felsic minerals to K-feldspar and illite-kaolinite, and alteration of mafic minerals to secondary biotite (Bt) and chlorite (Chl), pyrite (Py), hematite (Hm) and magnetite (Mt) in the East zone of the Red Chris deposit, northwestern British Columbia. Drillhole depths are shown in 200 m increments.

## Mineralization

Copper and gold grades in the East zone at Red Chris are concentrated in disseminated and vein-hosted bornite and chalcopyrite that are mostly within banded quartz-stockwork veins. Bornite and chalcopyrite are dominantly fine anhedral grains but locally form aggregates in quartz veins with minor to moderate white carbonate. Sulphide-only veins of chalcopyrite and/or bornite, 1–2 mm thick with wavy character, are particularly common in deeper portions of the N50E section line where K-silicate alteration dominates. Trace amounts of very fine grained chal-

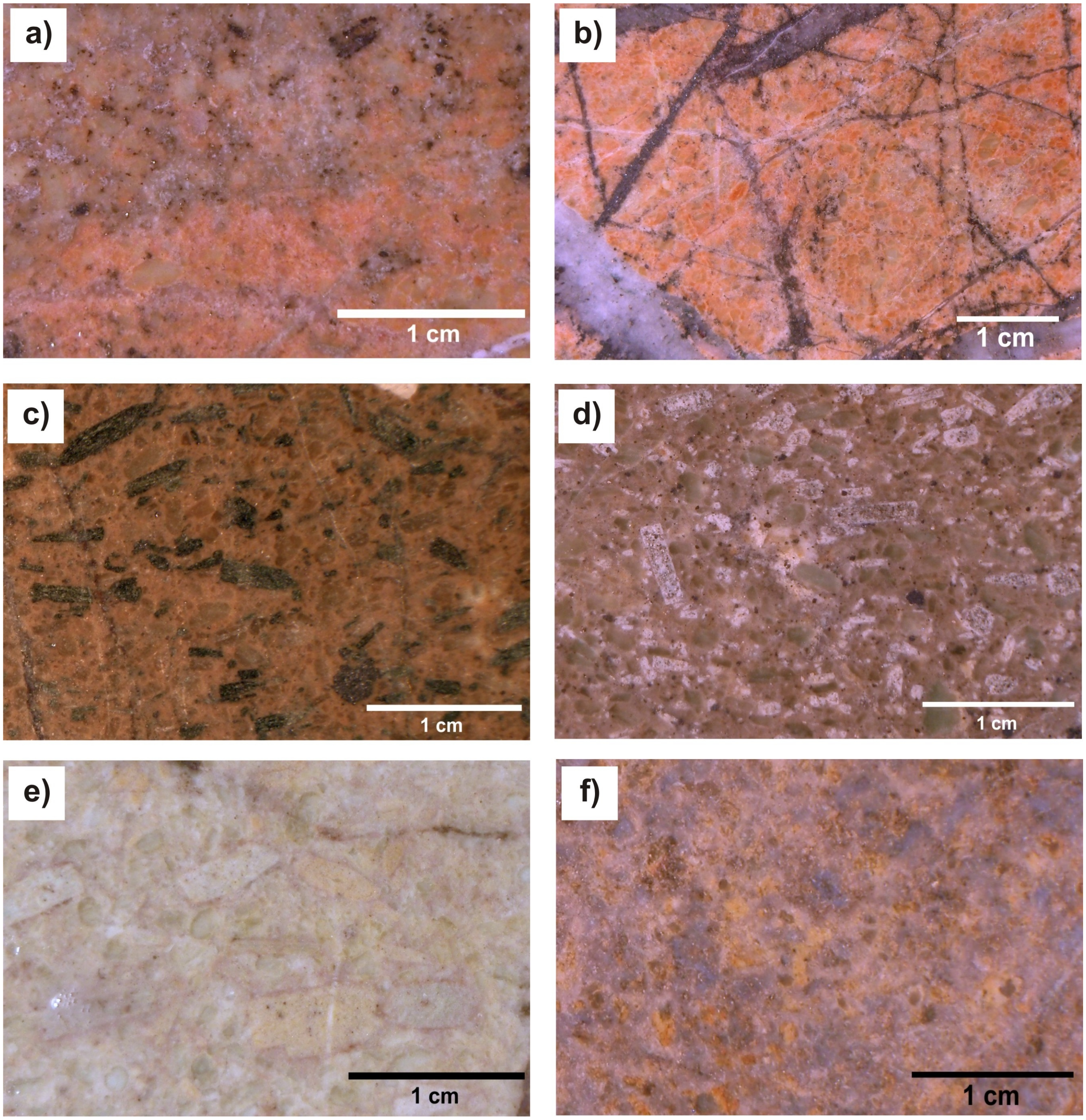


**Figure 6.** Typical examples of K-silicate and illite-kaolinite alteration in the Red stock from drillholes in the East zone of the Red Chris deposit, northwestern British Columbia: **a)** strong K-silicate alteration of monzodiorite, with mafic minerals altered to pyrite, hematite and illite-kaolinite, drillhole RC335-070 (985.37 m); **b)** intense K-silicate alteration of the groundmass with quartz veins, drillhole RC335-060 (863.54 m); **c)** K-silicate alteration of the groundmass, with secondary biotite phenocrysts (originally hornblende) being altered to magnetite and chlorite, drillhole RC335-034 (409.48 m); **d)** illite (light green) alteration of plagioclase phenocrysts and kaolinite (blotchy white) alteration of hornblende phenocrysts, drillhole RC335-041 (532.90 m); **e)** intense kaolinite and illite alteration of plagioclase and hornblende phenocrysts and of the groundmass, with the groundmass also being pervasively carbonate altered, drillhole RC335-035 (441.17 m); **f)** pervasive carbonate (ankerite?) alteration of plagioclase and hornblende phenocrysts (orange), along with intense carbonate alteration of the groundmass, drillhole RC106-019 (151.31 m). Figure reproduced from Norris et al. (2010).

copyrite are present in the K-silicate–altered mafic mineral sites and sparsely as fine-grained aggregates within purple anhydrite veins. Molybdenite is observed in minor and moderate amounts as fine- to medium-grained disseminations within quartz-carbonate veins and locally along the margins of quartz-carbonate±anhydrite veins.

Bornite, chalcopyrite, pyrite and molybdenite in quartz, quartz-carbonate and/or anhydrite veins have variable distributions along section N50E (Figure 7). A narrow, yet vertically significant zone of bornite+chalcopyrite occurs in the central region of the section, with its deepest extent at a depth of 1100 m in drillhole RC09-348. At 900 m in depth, this zone is roughly 200 m wide and was intersected by four adjacent drillholes. The bornite+chalcopyrite zone gradually narrows towards the surface, and is roughly 50 m wide at a depth of 50 m. Outboard of the bornite+chalcopyrite core, a zone of chalcopyrite>pyrite forms the bulk of the N50E section. A zone of pyrite>chalcopyrite in quartz veins forms an asymmetric dome about the centre of the section (drillholes RC09-348, RC07-335). This pyrite zone is concentrated near the surface in the western portion of the section and extends down to a depth of 400 m. Molybdenite occurs throughout the N50E section (typically <10 ppm) but is concentrated in moderate amounts (~50–100 ppm) in the eastern portion of the section below 750 m in depth.

Visual estimates of quartz-vein density across section N50E were recorded as percentages, divided into five bins (0–20%, 20–40%, 40–60%, 60–80% and 80–100%) and plotted as a histogram for each hole. Several isolated regions of quartz-vein densities greater than 20% cluster in the centre of the section and are outlined by thick black dashed lines on Figure 7. The widest region occurs in the centre of the East zone around 800 m in depth. A region of very high density of quartz veins occurs isolated within drillhole RC09-350 between 540 and 700 m in depth. Another region of very high density of quartz veins occurs at the surface and extending down to a depth of 65 m in drillholes RC07-335 and RC09-354.

## Grade

Copper and gold in the East zone at Red Chris have an average ratio of 1:1 (% Cu to g/t Au), and they are strongly correlated across all grades (coefficient of determination, $r^2$ = 0.89; Baker et al., 1999). Visible gold was not observed. Histograms of copper and gold grades across section N50E (Figure 7) show that the highest gold grades are associated with the highest densities of banded quartz-stockwork veins. The central section of the East zone has grades >0.5% Cu and >0.1 g/t Au from surface down to ~1000 m in depth, with localized sections of much higher grade values. The eastern portion of the section has grades typically >0.5% Cu and >0.1 g/t Au from 400–550 m down to ~1000 m, also with localized sections that are much higher in grade. An example is drillhole RC09-350, which has an intersection of 152 m, at 504 m in depth, of 4.12% Cu and 8.83 g/t Au. In the west (RC09-352), grades are typically >0.5% Cu and >0.1 g/t Au between depths of 400 and 850 m. The westernmost section of the East zone (RC09-351) has localized sections grading >0.5% Cu and >0.1 g/t Au between 400 and 800 m in depth. The highest gold grades are associated with the chalcopyrite and bornite core in the centre of the East zone, and locally outboard within areas of dominantly chalcopyrite. Copper and gold grade is controlled by quartz veins and does not appear to be related to one specific alteration association.

## Discussion and Conclusions

Although only one general compositional type of the Red stock was recognized by Schink (1977), changes in phenocryst size and abundance identified in this study indicate that several different porphyritic phases likely are present. The contacts between these different textural types are typically marked by zones of brecciation, which make crosscutting relationships difficult to determine. It is likely that the brecciated zones represent the original intrusive contacts between different porphyry units that were later reactivated by successive structural and fluid events, including deposition of the abundant late carbonate cement that is characteristic of these breccia zones. Some of these porphyry phases have much higher densities of veins and higher Cu and Au grades, and are interpreted to be early phases of the intrusion. Simple use of Cu and Au grades may therefore be useful, in addition to textural evidence, to distinguish between different porphyritic phases.

The typically high-grade mineralization at Red Chris is closely associated with areas that have multiple generations of the banded quartz-stockwork veins. Although most of the high-grade mineralization in the core of the East zone is chalcopyrite+bornite, the mineralization in the intense zone of quartz veining at a depth of 504 m in drillhole RC09-350 is almost entirely chalcopyrite. The distribution of high-density quartz veins may be lithologically controlled by compositionally similar yet paragenetically different porphyry intrusions.

Controls on the occurrence of hematite and magnetite remain ambiguous. The presence of hematite and magnetite in veins is directly associated with the K-silicate–altered core. However, the distribution of hematite and magnetite within mafic sites is irregular due to the intensity of the illite-kaolinite alteration overprint. Hornblende is altered to magnetite and secondary biotite locally within the K-silicate–altered zones, whereas mafic sites are altered to hematite within zones of the widespread illite-kaolinite alteration overprint. The fluids involved in the illite-kaolinite

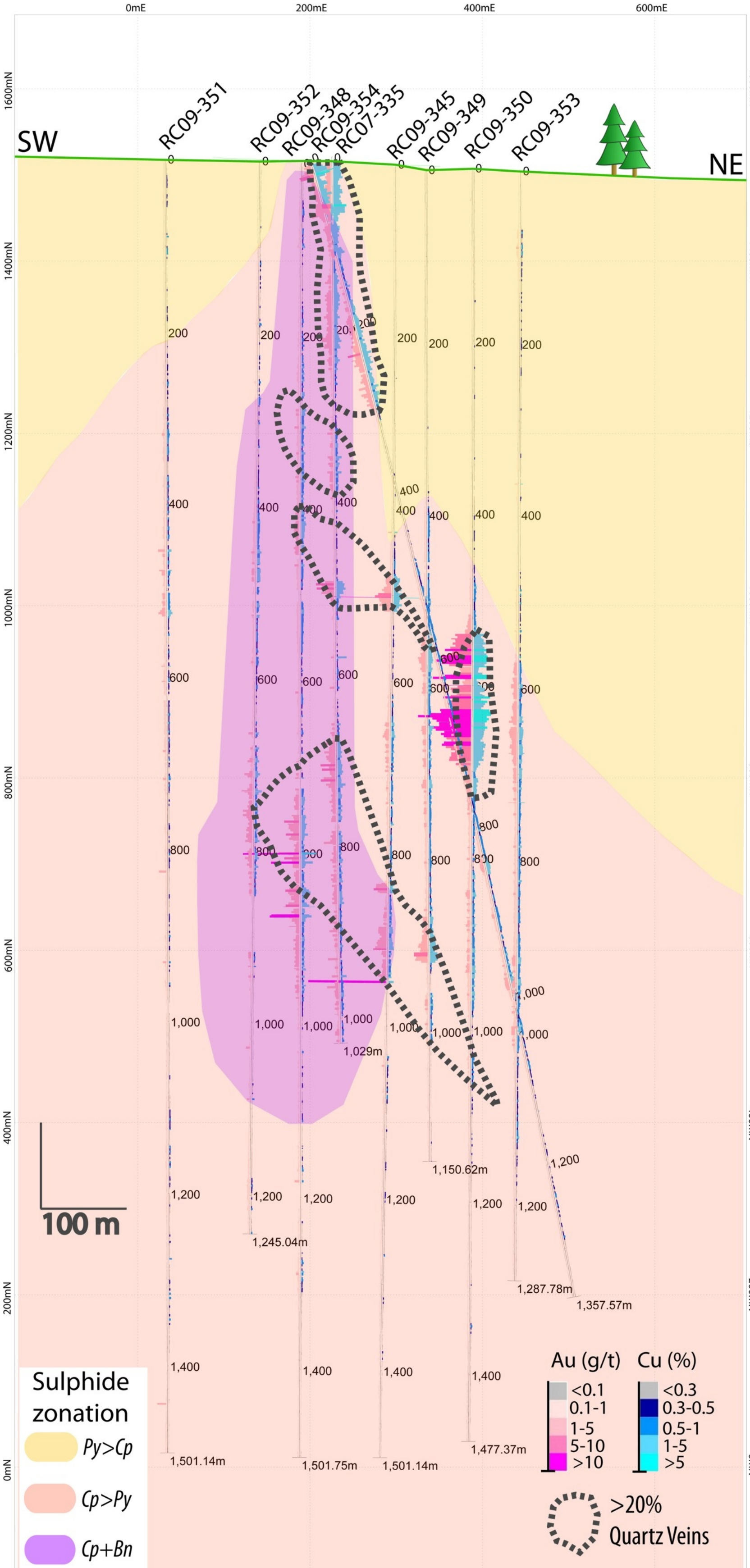

SW
NE
RC09-351
RC09-352
RC09-348
RC09-354
RC07-335
RC09-345
RC09-349
RC09-350
RC09-353
0mE
200mE
400mE
600mE
1600mN
1400mN
1200mN
1000mN
800mN
600mN
400mN
200mN
0mN
100 m
1,029m
1,150.62m
1,245.04m
1,287.78m
1,357.57m
1,501.14m
1,501.75m
1,477.37m
Sulphide zonation
Py>Cp
Cp>Py
Cp+Bn
Au (g/t)
<0.1
0.1-1
1-5
5-10
>10
Cu (%)
<0.3
0.3-0.5
0.5-1
1-5
>5
>20% Quartz Veins

alteration of the monzodiorite may have altered the magnetite to hematite.

The presence of illite and kaolinite as the dominant clay alteration minerals overprinting the K-silicate zone indicate a lower temperature association than the sericite mineral association. X-ray diffraction techniques will be used to confirm the results of the TerraSpec™ analyses and may indicate distinct muscovite-, illite- and kaolinite-dominant alteration zones.

Numerous crosscutting relationships between different vein types observed in the East zone complicate the development of a relative paragenesis. Fluids associated with individual porphyritic intrusions fractured older phases of the Red stock. Evolution of the magmatic compositions and their relationships to the veins, mineralization and alteration, and characterization of paragenetic vein sequences, are the focus of the next stage of research on the Red Chris deposit.

## Acknowledgments

Geoscience BC is acknowledged and thanked for the funding provided for this project. Imperial Metals Corporation is thanked for funding and wide-ranging support for the project; in particular, the support of S. Robertson and P. McAndless is appreciated. B. Clift, S. Ewanchuk, J. MacPherson, K. MacKenzie and A. Marko are also thanked for their input and discussion of the hostrocks and mineralization at Red Chris. The entire staff at the Red Chris camp, including T. Gainer, A. Robertson and N. Robertson, is thanked for help in moving countless core boxes. B. Riedell is thanked for stimulating conversations regarding the genesis of the deposit. A. Toma of the Mineral Deposit Research Unit at the University of British Columbia is thanked for logistical support. The peer review and suggestions given by F. Bouzari are greatly appreciated.

## References

Ash, C.H., Fraser, T.M., Blanchflower, J.D. and Thurston, B.G. (1995): Tatogga Lake project, northwestern British Columbia (104H/11, 12); *in* Geological Fieldwork 1994, BC Ministry of Forests, Mines and Lands, Paper 1995-1, p. 343–358.

Baker, T., Ash, C.H. and Thompson J.F.H. (1999): Geological setting and characteristics of the Red Chris copper-gold deposit, northwestern British Columbia; Exploration and Mining Geology, v. 6, no. 4, p. 297–316.

**Figure 7.** Cross-section of copper (%) and gold (g/t) grade (histogram), zonation of sulphide species (Bn, Cp, Py) and density of quartz veins >20% (visually estimated, outlined by thick dashed line) along the N50E section line of the East zone, Red Chris deposit, northwestern British Columbia.

Blanchflower, J.D. (1995): 1995 exploration report on the Red Chris property; unpublished report prepared for American Bullion Minerals Ltd., 93 p.

Collins, J., Colquhoun, W., Giroux, G.H., Nilsson, J.W. and Tenney, D. (2004): Technical report on the Red Chris copper-gold project, Liard Mining Division; unpublished company report, Red Chris Development Company Ltd.

Evenchick, C.A. and Thorkelson, D.J. (1993): Geology, Spatsizi River, British Columbia (104H); Geological Survey of Canada, Open File 2719, scale 1:250 000.

Ferreira, L. (2009): 2008 diamond drilling report on the Red Chris project located in northwest British Columbia, Liard Mining District; unpublished company report, Red Chris Development Company Ltd.

Friedman, R.M. and Ash, C.H. (1997): U-Pb age on intrusions related to porphyry Cu-Au mineralization in the Tatogga Lake area, northwestern British Columbia (104H/12NW, 104G/9NE); *in* Geological Fieldwork 1996, BC Ministry of Forests, Mines and Lands, Paper 1997-1, p. 291–298.

Gillstrom, G. and Robertson, S. (2010): Red Chris deposit technical report: 2010 exploration, drilling and mineral resource update; unpublished company report, Imperial Metals Corporation.

Giroux, G.H. and Bellamy, J. (2004): Update report on the Red Chris copper-gold project; unpublished company report, bcMetals Corporation.

Holliday, J.R. and Cooke, D.R. (2007): Advances in geological models and exploration methods for copper ± gold porphyry deposits; *in* Proceedings of Exploration 07: Fifth Decennial International Conference on Mineral Exploration, B. Milkereit (ed.), Prospectors and Developers Association of Canada, Toronto, Ontario, p. 791–809.

Imperial Metals Corporation (2007): Over one kilometre grading 1.01% copper and 1.26 g/t gold intercepted at Imperial's Red Chris property; Imperial Metals Corporation, press release, October 16, 2007, URL <http://www.imperialmetals.com/s/News-2007.asp> [November 2010].

Imperial Metals Corporation (2010): Imperial report results of the Red Chris feasibility study update; Imperial Metals Corporation, press release, November 16, 2010, URL<http://www.imperialmetals.com/s/News-2007.asp> [November 2010].

McMillan, W.J., Thompson, J.F.H., Hart, C.J.R. and Johnston, S.T. (1995): Regional geological and tectonic setting of porphyry deposits in British Columbia and Yukon Territory; *in* Porphyry Deposits of the Northwestern Cordillera of North America, T.G. Schroeter (ed.), Canadian Institute of Mining, Metallurgy and Petroleum, Special Volume 46, p. 40–57.

Meyer, C. and Hemley, J.J. (1967): Wall rock alteration; *in* Geochemistry of Hydrothermal Ore Deposits, H.L. Barnes (ed.), Holt, Reinhart and Winston, New York, p. 166–235.

Monger, J. and Price, R. (2002): The Canadian cordillera: geology and tectonic evolution; Canadian Society of Exploration Geophysicists Recorder, v. 27, no. 2, p. 17–36.

Newell, J.M. and Peatfield, G.R. (1995): The Red-Chris porphyry copper-gold deposit, northwestern British Columbia; *in* Porphyry Deposits of the Northwestern Cordillera of North America, T.G. Schroeter (ed.), Canadian Institute of Mining, Metallurgy and Petroleum, Special Volume 46, p. 674–688.

Norris, J.R., Hart, C.J.R., Tosdal, R.M. and Rees, C. (2010): Preliminary study of the magmatic evolution, mineralization and alteration at the Red Chris copper-gold porphyry deposit, northwestern British Columbia (NTS 104H/12 W); *in* Geoscience BC Summary of Activities 2009, Geoscience BC, Report 2010-1, p.77–86., URL <http://www.geosciencebc.com/s/SummaryofActivities.asp?ReportID=379075> [November 2010].

Schink, E.A. (1977): Geology of the Red Chris porphyry copper deposit, northwestern British Columbia; M.Sc. thesis, Queens University, Kingston, Ontario, 211 p.

Seedorff, E., Dilles, J.H., Proffett, J.M., Einaudi, M.T., Zurcher, L., Stavast, W.J.A., Barton, M.D. and Johnson, D.A. (2005): Porphyry-related deposits: characteristics and origin of hypogene features; *in* Economic Geology, 100th Anniversary Volume, p. 251–298.